PHYSICAL REVIEW B VOLUME 32, NUMBER 12 15 DECEMBER 1985

# Unoccupied-state electronic structure in $(Ni_yPt_{1-y})_{75}P_{25}$ and $Ni_{100-x}P_x$ metallic glasses

M. Choi, D. M. Pease, W. A. Hines, G. H. Hayes, and J. I. Budnick
*Department of Physics and Institute of Materials Science, University of Connecticut, Storrs, Connecticut 06268*

S. M. Heald
*Brookhaven National Laboratory, Upton, New York 11973*

R. Hasegawa
*Allied Corporation, Morristown, New Jersey 07960*

H. E. Schone
*Department of Physics, College of William and Mary, Williamsburg, Virginia 23186*
(Received 19 August 1985)

The $L_{III,II}$-edge x-ray absorption near-edge structure (XANES) of Pt and the $K$-edge XANES of Ni have been measured for the amorphous $(Ni_yPt_{1-y})_{75}P_{25}$ system. The Ni-$K$-edge XANES in roller-quenched amorphous $Ni_{100-x}P_x$, and Ni-$L_{III}$-edge XANES in electrodeposited amorphous $Ni_{100-x}P_x$ have also been obtained. Results on $(Ni_yPt_{1-y})_{75}P_{25}$ agree qualitatively with expectations based on recent relativistic Korringa-Kohn-Rostoker coherent-potential-approximation (KKR-CPA) calculations for $Ni_xPt_{1-x}$ solid solutions. Similar agreement is found between our experimental results on $Ni_{100-x}P_x$ and recent KKR-CPA calculations for this system. No evidence is found for Pt or Ni $d$-hole filling in any of these metallic glasses. Finally, our results on electrodeposited $Ni_{100-x}P_x$ are similar to previous measurements on chemically deposited $Ni_{80}P_{20}$ carried out by others.

## I. INTRODUCTION

Transition-metal plus metalloid (TM-$M$) metallic glasses are studied by a number of techniques which measure the density of $d$ states at the Fermi level, $\rho_d(E_F)$. It is commonly found in such measurements that $\rho_d(E_F)$ is sharply reduced in the glass relative to its value in the pure transition metal,[1-6] and the observation of such a lowering of $\rho_d(E_F)$ is often interpreted as evidence for a filling of the TM $d$ band in these systems.[1-6] Recently, however, Pease *et al.* pointed out that the x-ray absorption near-edge structure (XANES) of a number of TM-$M$ glasses and related crystalline alloys shows little evidence for $d$-band filling. In addition, these authors found that the number of local Pt $5d$ holes per Pt site in a $(Ni_{0.50}Pt_{0.50})_{75}P_{25}$ metallic glass actually *increases* in the alloy relative to pure Pt; whereas for the alloy, Hines *et al.* had by measurements of the Pt Knight shift previously demonstrated a *decrease* in the $\rho_d(E_F)$ of local Pt sites.[6,7] Pease *et al.* discussed a model for resolving such apparently contradictory results.[7] In this picture, the addition of metalloid atoms does result in an energy broadening of the $d$-hole distribution and a lowered $\rho_d(E_F)$; however, because of the inherent core-hole lifetime broadening of XANES, the latter type of experiment does not resolve the changes in $\rho_d(E_F)$. Rather, XANES is sensitive to the total $d$-hole count, and the integrated number of local $d$ holes per TM site in these alloys is not found to decrease relative to that of the pure transition metal.

In the present work, systematics in the XANES of different compositions of amorphous $(Ni_xPt_{1-x})_{75}P_{25}$ and $Ni_{100-x}P_x$ glasses have been observed. The results further support the general conclusion that the presence of metalloid atoms does not result in the filling of transition-metal $d$ holes. Furthermore, the results are in qualitative agreement with recent one-electron band-structure calculations on related systems.[8,9]

The present studies of the amorphous $Ni_{100-x}P_x$ system are of interest for reasons outside the domain of the context discussed above. The Ni $L_{III}$ XANES of chemically deposited, amorphous $Ni_{80}P_{20}$ has been previously measured by Belin *et al.*;[10] at the same time, there is strong evidence from phosphorous Knight-shift measurements for significant differences between the $s$-character electronic structure of chemically deposited versus electrodeposited amorphous Ni-P,[11] and for a corresponding polymorphism in this system. Thus, we have measured the Ni $L_{III}$ XANES of a series of electrodeposited $Ni_{100-x}P_x$ amorphous alloys and compared our results to the previous work on the chemically deposited system by Belin *et al.*,[10] in order to search for corresponding differences in the Ni $3d$ electronic structure between these two types of amorphous Ni-P.

## II. EXPERIMENTAL APPARATUS AND PROCEDURE

As a general rule, the optimum sample thickness for transmission XANES is such that the thickness $t$ of the element whose edge is being measured is of the order $2/\mu$, where $\mu$ is the linear absorption coefficient on the high absorbing side of the absorption edge. Thus, for Ni $L_{III}$ edges, samples should be of the order of 1000 Å in thickness, and for Ni $K$ and Pt $L$ edges, sample thicknesses should be roughly 10 $\mu$m or less. For the Ni-$K$-edge

 

XANES in $Ni_{100-x}P_x$, samples were polished down from a roller-quenched ribbon using a polishing wheel and a special thin-foil mounting device developed by one of us (M.C.). On the other hand, it was not possible to polish mechanically samples which were sufficiently thin for Ni $L$-edge work. These samples were fabricated using a procedure described as follows. First, a copper film was evaporated onto a specially thinned polypropylene sheet. During the evaporation the polypropylene was cooled from in back by contact with a water-cooled, convex copper block. The $Ni_{100-x}P_x$ alloy was then electrodeposited onto the vacuum-deposited copper film. Electrical contact was made using conducting paint, and the electrodeposition was carried out using Brenner's bath as described by Cargill.[12,13] The $(Ni_yPt_{1-y})_{75}P_{25}$ samples were splat-quenched foils that were not suitable for mechanical thinning. However, it was possible to find small areas on the edges of these foils which were sufficiently thin for the Pt-$L$-edge and Ni-$K$-edge XANES measurements, yet were pinhole free. These regions were carefully masked off with lead, and although the resulting areas were too small for use in a laboratory spectrometer, the large intensities available with a synchrotron source insured that the resulting sample areas were sufficient. Roller-quenched and splat-quenched foils were characterized by x-ray diffraction to insure their amorphous nature, and by chemical analysis to check the chemical composition. Electrodeposited $Ni_{100-x}P_x$ samples were characterized by two different techniques. First, thin electrodeposited samples were chemically analyzed by atomic absorption (nickel) and colorimetry (phosphorous) by a certified testing laboratory. Corresponding thick samples were built up on copper substrates by longer electrodeposition times. These bulk samples were analyzed using a microprobe and by means of x-ray diffraction. The analyzed phosphorous content of the thin-film samples consistently exceeded that of the bulk samples, as analyzed by microprobe, by 2—3 at. %. Since the type of analysis used for the thin films also gave a phosphorous composition higher, by approximately 3 at. % than the known composition of a bulk test standard, the microprobe results were used in assigning the most accurate nominal compositions to the thin $Ni_{100-x}P_x$ films. X-ray diffraction of the 25—at. %—P phosphorous sample revealed only the expected broad diffraction peaks characteristic of an amorphous structure. Cargill's results imply that for phosphorous concentrations in the range of 11 at. % or lower, electrodeposited $Ni_{100-x}P_x$ exhibits an interesting diffraction pattern with traces of broad peaks corresponding to Ni in a (111) fiber texture.[12] In the present study, traces of such a fiber texture are also observed for the two samples of lower phosphorous composition. As will be seen, the Ni $L_{III}$ XANES of the electrodeposited $Ni_{100-x}P_x$ system exhibits a systematic concentration dependence of the XANES, despite the evidence for differences in structure between low- and high-phosphorous-containing samples.

The x-ray absorption spectra were obtained on two different kinds of facilities. The K edges of Ni and $L$ edges of Pt were obtained using the $C2$ beam line of the Cornell High Energy Synchrotron Source (CHESS) facility (Cornell University, Ithaca, New York). A channel-cut silicon monochromator crystal with a (220) cut was used, and the resolution is estimated to be on the order of 2 eV. The $L$-edge spectra of Ni were obtained using a double-crystal laboratory vacuum instrument described by Gregory and Best.[14] Rubidium acid pthatalate (RAP) crystals were used, with a resolution at the Ni $L$ edge of approximately 1.8 eV. The double-crystal spectrometer was operated in a "$\theta-3\theta$" mode. In this method of operation, the first crystal is moved by a change in angle $\Delta\theta$, and the second crystal is moved in the same rotation direction as the first, but by $3\Delta\theta$, in order to change the effective Bragg angle by $\Delta\theta$. This method of operation makes possible certain simplifications in the operation of a double-crystal laboratory spectrometer, and will be described elsewhere.[15]

Finally, in terms of instrumental errors, the "x-ray thickness effect" is of importance.[16,17] For the data taken with the synchrotron, it was found that varying the thickness of sample absorbers did not effect the shape of the XANES spectra, and that thickness effects could therefore be considered negligible for the Ni $K$ and Pt $L_{III,II}$ absorption edges. The Ni $L_{III}$ edges taken with the laboratory vacuum spectrometer showed the usual large thickness effects and the calibration method described by Pease[17] was used to separate electronic structure from sample thickness effects on the spectra. In addition to the fact that the synchrotron data were free from thickness-effect distortions, it might be mentioned that excellent XANES spectra were taken in a few seconds per sample using the hard-x-ray synchrotron beam, whereas the laboratory soft-x-ray data required a continuous running time of approximately a week.

## III. RESULTS

The Pt $L_{III}$ and $L_{II}$ edges in pure Pt and three compositions of $(Ni_yPt_{1-y})_{75}P_{25}$ are shown in Figs. 1. and 2. There is a negligible effect on the $L_{III}$-edge peak maximum due to varying the Ni to Pt ratio. All the alloys have an $L_{III}$-edge maximum, or "white-line," which is slightly lowered and broadened relative to that of pure Pt. On the other hand, there are small, but definite systematic changes in the shape of the Pt-$L_{II}$-edge spectra as the Ni to Pt ratio is changed. The area under the threshold region of the $L_{II}$ XANES is larger for each alloy than for pure Pt, and the increase of the Pt to Ni ratio systematically flattens and lowers the $L_{II}$ XANES peak. [In the previous study of the one $(Ni_{50}Pt_{50})_{75}P_{25}$ composition, a small pre-edge dip was detected.[7] No discussion of this feature was then made because of the possibility of an instrumental artifact. This pre-edge feature did not appear in a subsequent synchrotron run, although other features of the spectra were reproduced.]

The Ni $L_{III}$-edge spectra of electrodeposited $Ni_{100-x}P_x$ are shown in Fig. 3, along with Ni $L_{III}$ edges for several thicknesses of pure Ni. It is evident that the addition of phosphorous has two pronounced effects on the spectra. (1) The peak of the absorption white line, and consequent location of the Fermi level, is shifted to higher energies as the P content increases. (2) Relative to the pure Ni case, the average value of the absorption coefficient does not

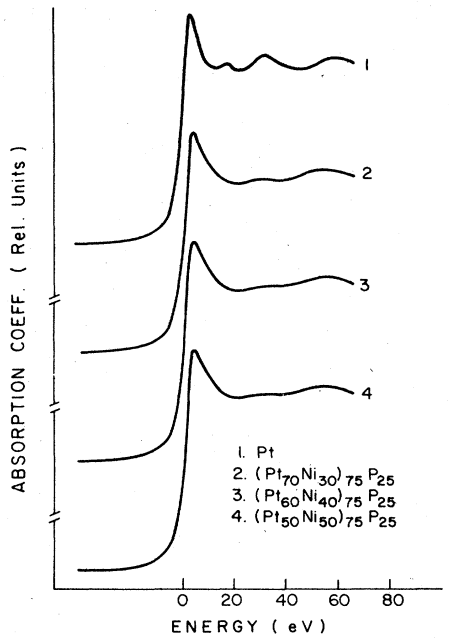


FIG. 1. Pt-$L_{III}$-edge XANES for amorphous $(Ni_xPt_{100-x})_{75}P_{25}$ and pure Pt. The spectra are normalized by subtracting the pre-edge background and then normalizing to a node in the extended x-ray absorption fine-structure (EXAFS) region.

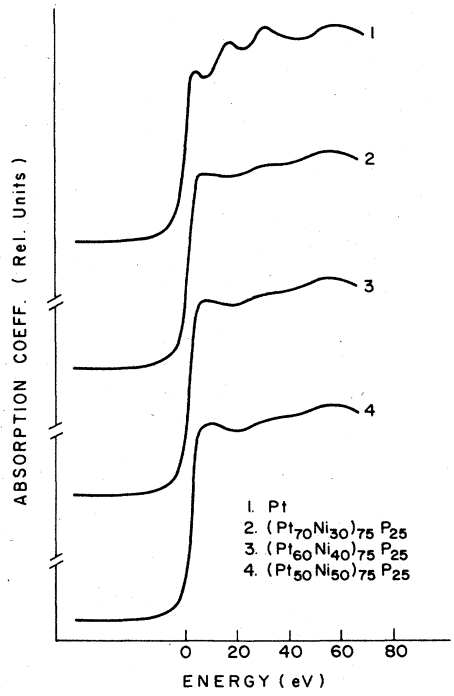


FIG. 2. Pt-$L_{II}$-edge XANES for amorphous $(Ni_xPt_{100-x})_{75}P_{25}$ and pure Pt. The spectra are normalized by subtracting the pre-edge background and then normalizing to a node in the EXAFS region.

flatten out so quickly for energies greater than that corresponding to the absorption peak. Pease has developed a method for separating thickness-effect distortions from true effects of alloying on electronic structure, by means of a calibration curve which utilizes different thicknesses of pure calibrations samples.[17] Figure 4 shows such a thickness-effect calibration curve for the data in Fig. 3. If thickness effects are accounted for, there is no discernable effect of alloying on the relative height of the Ni white-line maximum, as is evident from the fact that pure Ni and metallic glass samples all plot smoothly on the same thickness-effect calibration curve.

Figure 5 illustrates the comparative shape of the Ni-$K$-edge XANES of pure Ni, roller-quenched $Ni_{80}P_{20}$, and two compositions of $(Ni_yPt_{1-y})_{75}P_{25}$. It may be seen that the near-edge structure in the $Ni_{80}P_{20}$ alloy is largely washed out compared to that of pure Ni. There is some structure in the Ni XANES of the Pt-containing metallic glasses, however, which looks quite different from that of $Ni_{80}Pt_{20}$. There appears to be systematic enhancement of this structure as the Pt to Ni ratio increases.

## IV. DISCUSSION AND CONCLUSIONS

### A. Pt $L$ edges in amorphous $(Ni_yPt_{1-y})_{75}P_{25}$

Brown *et al.* did an experimental-theoretical study of the pure Pt XANES and pointed out that there is a sharp white-line maximum for the Pt $L_{III}$, but not the $L_{II}$, edge.[18] This observation indicates that there are predominantly $5d_{5/2}$ holes, and few $5d_{3/2}$ holes, just above the Fermi level in pure Pt. A calculation of the band struc-

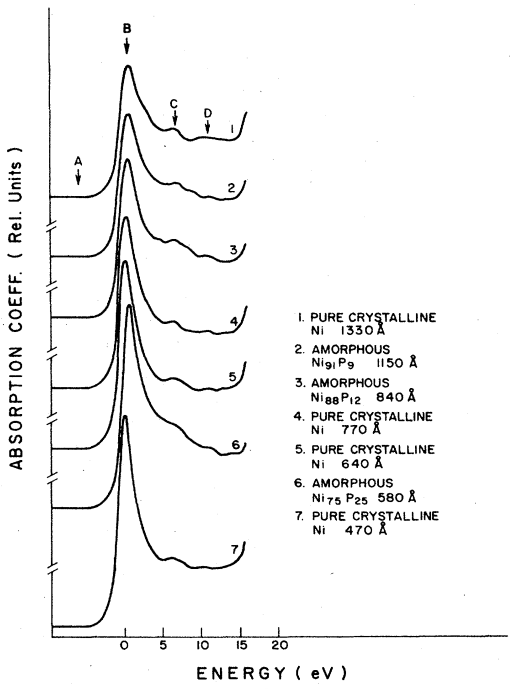


FIG. 3. Ni-$L_{III}$-edge XANES for amorphous, electrodeposited $N_{100-x}P_x$ and pure Ni. These spectra have been normalized by setting the $\mu_D - \mu_A$ value for each sample equal to one.

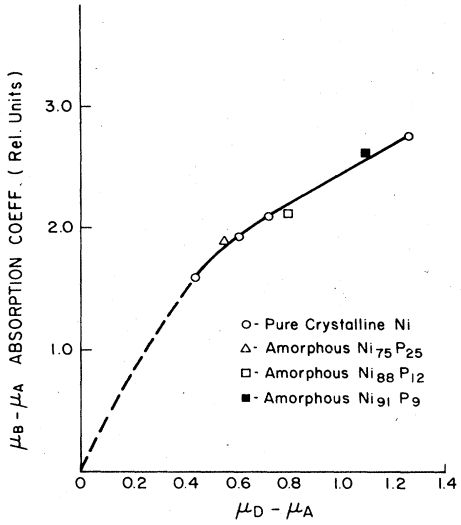


FIG. 4. Thickness-effect calibration curve, Ni $L_{III}$ edge. The raw-data values of $\mu_B - \mu_A$ are plotted versus the raw-data values of $\mu_D - \mu_A$.

ture of pure Pt by Mattheiss and Deitz[19] confirms the arguments of Brown *et al.*[18]

Recently, Staunton, Weinberger, and Gyorffy have performed relativistic Korringa-Kohn-Rostoker coherent-potential-approximation (KKR-CPA) calculations for $Ni_xPt_{1-x}$ random solid solutions.[8] Figure 6 illustrates the decomposition of the number of local Pt unoccupied $5d_{5/2}$ and $5d_{3/2}$ states per Pt site in $Ni_{50}Pt_{50}$, as taken

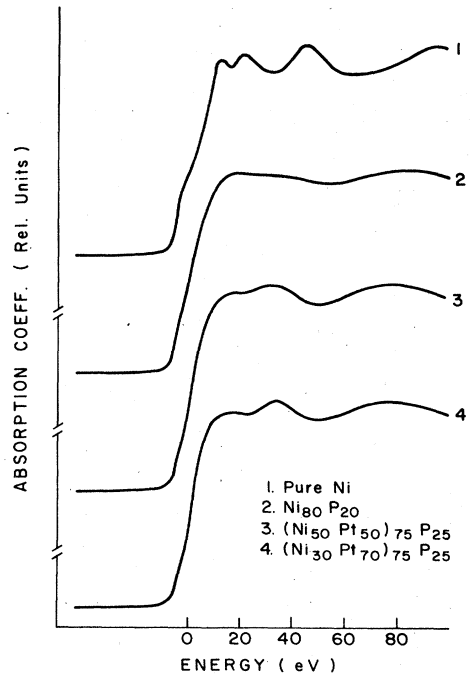


FIG. 5. Ni-*K*-edge XANES spectra for pure Ni, roller-quenched amorphous $Ni_{80}P_{20}$, and amorphous $(Ni_xPt_{100-x})_{75}P_{25}$. The spectra are normalized by subtracting the pre-edge background and then normalizing to a node in the EXAFS region.

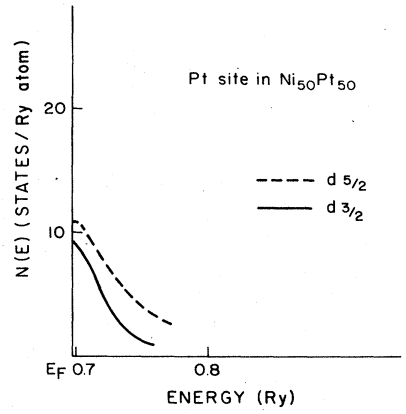


FIG. 6. Theoretical Pt $d_{5/2}$ and $d_{3/2}$ unoccupied-state density versus energy curves for $Ni_{50}Pt_{50}$, adapted from Ref. 8. The energy scale is referenced with respect to the muffin-tin zero.

from Staunton *et al.*[8] For comparison, Fig. 7 shows a plot of the unoccupied $d_{3/2}$ and $d_{5/2}$ states for pure Pt, taken from Mattheiss and Dietz.[19]

Certain general trends are evident from a comparison of Figs. 6 and 7. First, for both pure Pt and $Pt_{50}Ni_{50}$, the number of $d_{5/2}$ holes per Pt site is predicted to exceed the number of $d_{3/2}$ holes. Second, it is evident that the theoretical ratio between the number of $d_{5/2}$ to $d_{3/2}$ holes is less for the $Ni_{50}Pt_{50}$ random solid solution than for pure Pt. There is, therefore, theoretical evidence that the addition of Ni decreases the large difference between the number of $d_{5/2}$ and $d_{3/2}$ holes per Pt site, relative to the case of pure Pt.

These theoretical predictions are supported by the data on the $(Ni_yPt_{1-y})_{75}P_{25}$ system. In all of these alloys, the area under the threshold region of the Pt $L_{II}$ edge is less than the corresponding area under the $L_{III}$-edge maximum, just as in the case for pure Pt. On the other hand, the area under the threshold region of the Pt $L_{II}$ edge is greater for all the alloys than for pure Pt. This observation is in general agreement with expectations based on comparisons of the calculations for Pt and for $Pt_xNi_{1-x}$. Of most significance is the experimental observation that

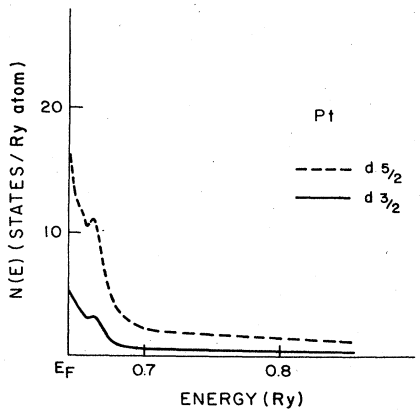


FIG. 7. Theoretical Pt $d_{5/2}$ and $d_{3/2}$ unoccupied-state density versus energy curves for pure Pt, adapted from Ref. 19. The energy scale is referenced with respect to the muffin-tin zero.

there is definite depression of the Pt-$L_{II}$-edge peak in the metallic glass upon increasing the Pt to Ni ratio. This systematic depression of the threshold Pt-$L_{II}$-edge maximum adds strong support to the above interpretation of our data in terms of a comparison of the theoretical results for pure Pt and for $Pt_{50}Ni_{50}$. It is of interest that the effect of changing the Pt to Ni ratio is rather small in the concentration region studied here. One might guess that in the Pt-rich regime, quite small additions of Ni would have a drastic effect on the $d_{3/2}$- to $d_{5/2}$-hole ratio. This last conjecture would be interesting to test experimentally. Finally, it would also be of interest to perform experiments on other systems to see if, in general, the addition of first-row transition metals (which have "nonrelativistic" band structures) reduces the relativistic spin-orbit effects found in the $d$ holes of heavy-metal systems such as Pt.

### B. Ni $L_{III}$ edges in amorphous $N_{100-x}P_x$

Lashmore *et al.* compared the results of phosphorous Knight-shift measurements in electrodeposited and chemically deposited amorphous Ni-P. These authors found evidence of significantly greater phosphorous $s$ character at the Fermi level for the chemically deposited relative to the electrodeposited material.[11] Subsequently, Belin *et al.* measured the $L_{III}$ Ni XANES of chemically deposited $Ni_{80}P_{20}$.[10] They observed a shift to higher energies of the initial inflection point relative to pure Ni, and a pronounced broadening of the Ni $L_{III}$ XANES. For the one amorphous sample and one Ni sample studied, there was a decrease in the relative height of the Ni white line in the alloy relative to that of pure metal. As far as a general comparison is concerned, our results on electrodeposited $Ni_{100-x}P_x$ show a similarity to those previously observed for the chemically deposited alloy. A pronounced broadening is observed, as is a shift to higher energies of the threshold maximum with phosphorous addition. Our thickness-effect calibration curve, however, shows no diminution of the relative height of the $3d$-hole white line relative to the pure Ni case. Our two compositions of lower phosphorous concentration yield XANES with the same general characteristics as that of the fully amorphous $Ni_{75}P_{25}$ sample; however, the magnitude of the high-energy shift to the threshold maximum is less. As discussed above, the diffraction pattern of our phosphorous-poor compositions is characterized by an admixture of "fiber-texture" diffraction peaks, whereas our most phosphorous-rich sample appears to be totally amorphous. Thus, our results, taken together with the work by Lashmore *et al.*[11] and Belin *et al.*[10] on chemically deposited $Ni_{80}P_{20}$, indicate that there is a structure insensitivity in the distribution of unoccupied $d$ states in the $Ni_{100-x}P_x$ system.

Our results show no evidence for $d$-band filling in the $Ni_{100-x}P_x$ system. There is evidence for qualitative agreement with recent calculations, in this regard. Recently, Khanna *et al.* have calculated the electronic structure of a $Ni_{74}P_{26}$ metallic glass by a method based on the KKR-CPA approach.[9] The Fermi level is found to be in the $d$ band, in agreement with the XANES results on both the electrodeposited and chemically deposited systems. The calculated density of states at the Fermi level is lowered in the glass relative to pure Ni, in agreement with measurements that are sensitive to that quantity;[5] on the other hand, the Ni $d$-hole region is broadened relative to that of pure Ni, so that the lowering of $\rho_d(E_F)$ does *not* imply a consequent filling of Ni $3d$ holes.

With respect to the similarity of the XANES results for the $d$ holes of electrodeposited and chemically deposited $Ni_{100-x}P_x$, it may be of importance that the phosphorous Knight-shift experiments measure directly states of $s$, rather than $d$ symmetry. Whereas probes of TM $d$ bands have generally indicated a certain degree of structure insensitivity, this has not been the case for probes of states of other symmetry. Thus, Dose and Haertl observed a pronounced effect of atomic structure on the $s$, but not $d$ symmetry states in the appearance potential spectra of $Co_{58}Ni_{10}Fe_5B_{16}Si_{11}$.[20] Therefore, the kind of electronic structure differences observed by NMR between electrodeposited and chemically deposited $Ni_{100-x}P_x$ may not imply consequent changes in the local Ni $3d$ holes.

### C. Ni $K$ edges

As far as the Ni-$K$-edge XANES is concerned, the most striking observation is the smoothing of the $K$-edge XANES in amorphous $Ni_{80}P_{20}$. This result is not unexpected, in that both structural and chemical disorder have been shown to have a pronounced smoothing effect on $K$-edge XANES of similar systems. Pease *et al.* have combined XANES measurements on Al containing TM-based random solid solutions with average T-matrix approximation calculations of the band structure.[21] Addition of aluminum was theoretically predicted to produce a pronounced chemical disorder smearing of the TM-based electronic structure, and the predicted smearing was observed in the XANES. Similarly, Wong *et al.* have shown that the $K$-edge XANES of $Ni_{75}B_{25}$ shows smearing due to structural disorder when this substance goes from the crystalline to the amorphous state.[22] Both structural and chemical disorder should therefore be at work to smear the $K$-edge XANES of $Ni_{100-x}P_x$ relative to that of pure Ni. The $K$-edge XANES of Ni in the $(Ni_yPt_{1-y})_{75}P_{25}$ system, however, is difficult to interpret. It is interesting that the appearance of this spectrum is *much* different than that of Ni in $Ni_{100-x}P_x$, and the disorder smearing effects appear to be less. However, speculations on the origin of the large changes in the Ni $K$ XANES which are caused by the presence of Pt atoms would be premature at the present time.

Taken together, it may be concluded that the results discussed in IV A, IV B, and IV C add support to the model presented in Ref. 7. In this picture, the often observed lowering of $\rho_d(E_F)$ in amorphous systems due to metalloid addition is attributed, not to a filling of TM $d$ holes, but to a redistribution of the density of states above the Fermi energy such that the Fermi energy is either near a minimum in $\rho_d(E_F)$ or bordering on a broad "tail" of $d$-hole density. Usually, as in the present study, the core-hole broadening of XANES is larger than the extent of the $d$-hole redistribution, so that only a kind of integrated

$d$-hole count is observed and the detailed distribution of the $d$ holes is not detected. One therefore looks for supporting evidence for the above picture such as is presented here, in that the XANES results agree qualitatively with careful band-structure calculations for related crystalline alloys. In retrospect, however, there has been at least one XANES study in which the $d$-hole redistribution introduced by the metalloid in a related crystalline alloy was so large that details of this structure were experimentally resolved in the XANES, and it is perhaps not amiss to mention this result in the present context. The Ni $L_{III}$ XANES of $Ni_{50}Al_{50}$ ordered alloys shows a clear splitting of the Ni white line.[23] At the time the results on $Ni_{50}Al_{50}$ were published, comparisons were only possible with total-density-of-states calculations. Recently, however, projected $d$-component densities of states for this alloy have become available.[24] It is now clear that the high-energy, split-off component of the Ni white line in the XANES is largely of $d$ symmetry, so that in this case at least, XANES was able experimentally to resolve the details in the high-energy redistribution of TM $d$ holes due to metalloid addition.

## ACKNOWLEDGMENTS

We are grateful to Stanley Manter and his co-workers in the Institute of Materials Science (IMS), University of Connecticut, machine shop, and to Gary Moebus and his co-workers in the IMS electrical shop, without whose help this project could not have been completed. We are also grateful to Eva Rand for performing the microprobe analysis. The contributions of one of us (M.C.) are from material submitted in partial fulfillment of the requirements of the Ph. D. degree at the University of Connecticut. This research was supported by the U.S. Department of Energy (Contract No. DE-AS05-80ER10742) as part of a development program for beam line X-11 A at the National Synchrotron Light Source at Brookhaven National Laboratory, which is supported by the U.S. Department of Energy, Division of Materials Sciences and Division of Chemical Sciences under Contract No. DE-AC02-76CH00016. Support was also received from the Connecticut Research Foundation. One of us (W.A.H.) was supported by the U.S. Air Force Office of Scientific Research, Contract No. 80-0030.

[1]S. R. Nagel, G. B. Fisher, J. Tauc, and B. G. Bagley, Phys. Rev. B **13**, 3284 (1976).

[2]B. G. Bagley and F. J. DiSalvo, in *Amorphous Magnetism*, edited by H. O. Hooper and A. M. de Graaf (Plenum, New York, 1973), p. 143.

[3]B. Golding, B. G. Bagley, and F. S. L. Hsu, Phys. Rev. Lett. **29**, 68 (1972).

[4]J. D. Riley, L. Ley, J. Azoulay, and K. Terakura, Phys. Rev. B **20**, 776 (1979).

[5]W. A. Hines, C. V. Modzelewski, R. N. Paolino, and R. Hasegawa, Solid State Commun. **39**, 699 (1981).

[6]W. A. Hines, L. T. Kabacoff, R. Hasegawa, and P. Duwez, in *Amorphous Magnetism*, edited by R. A. Levy and R. Hasegawa (Plenum, New York, 1977), p. 207.

[7]D. M. Pease, G. H. Hayes, M. Choi, J. I. Budnick, W. A. Hines, R. Hasegawa, and S. M. Heald, J. Non-Cryst. Solids **62**, 1359 (1984).

[8]J. J. Staunton, P. Weinberger, and B. L. Gyorffy, J. Phys. F **13**, 779 (1983).

[9]S. N. Khanna, A. K. Ibrahim, S. W. McKnight, and A. Bansil (unpublished).

[10]E. Belin, C. Bonnelle, J. Flechon, and F. Machizoud, J. Non-Cryst. Solids **41**, 219 (1980).

[11]D. S. Lashmore, L. H. Benner, H. E. Schone, P. Gustafson, and R. E. Watson, Phys. Rev. Lett. **48**, 1760 (1982).

[12]G. S. Cargill III, J. Appl. Phys. **41**, 12 (1970).

[13]A. Brenner, *Electrodeposition of Alloys, Principles and Practice* (Academic, New York, 1963), Chap. 35.

[14]T. K. Gregory, and P. E. Best, Adv. X-Ray Anal. **15**, 90 (1971).

[15]D. M. Pease (unpublished).

[16]L. G. Parratt, C. F. Hempstead, and E. L. Jossen, Phys. Rev. **150**, 1228 (1957).

[17]D. M. Pease, Appl. Spectrosc. **30**, 405 (1976).

[18]M. Brown, R. E. Peierls, and E. A. Stern, Phys. Rev. B **15**, 738 (1977).

[19]L. F. Mattheiss and R. E. Dietz, Phys. Rev. B **22**, 1663 (1980).

[20]V. Dose and A. Haertl, Phys. Rev. Lett. **47**, 132 (1981).

[21]D. M. Pease, F. Szmulowicz, and L. V. Azaroff, Phys. Lett. **101A**, 38 (1984).

[22]J. Wong and H. Lieberman, Phys. Rev. B **29**, 651 (1984).

[23]D. M. Pease and L. V. Azaroff, J. Appl. Phys. **50**, 6605 (1979).

[24]C. Muller, W. Blau, and P. Zieche, Phys. Status Solidi B **116**, 561 (1983).